

Inversion of P-wave nonhyperbolic moveout in azimuthally anisotropic media: Methodology and field-data application

Ivan Vasconcelos and Ilya Tsvankin, *Center for Wave Phenomena, Department of Geophysics, Colorado School of Mines*

Summary

The azimuthally varying nonhyperbolic moveout of P-waves in orthorhombic media can provide valuable information for characterization of fractured reservoirs and seismic processing. Here, we present a technique to invert long-spread, wide-azimuth P-wave data for the orientation of the vertical symmetry planes and five key moveout parameters – the symmetry-plane NMO velocities $V_{\text{nmo}}^{(1)}$ and $V_{\text{nmo}}^{(2)}$ and the anellipticity parameters $\eta^{(1)}$, $\eta^{(2)}$, and $\eta^{(3)}$. The inversion algorithm is based on a 3D semblance operator applied to the full range of offsets and azimuths using a generalized version of the Alkhalifah-Tsvankin nonhyperbolic moveout equation. Numerical tests on noise-contaminated data show that the inversion yields satisfactory results if the offset-to-depth ratio reaches at least 2.5.

The algorithm was successfully tested on wide-azimuth P-wave reflections recorded at Weyburn Field in Canada. Taking azimuthal anisotropy into account increased the semblance values for most long-offset reflection events in the overburden, which indicates that fracturing is not limited to the reservoir level. The estimated symmetry-plane directions are close to the azimuths of the off-trend fracture sets determined from borehole data and shear-wave splitting analysis. The effective moveout parameters estimated by our algorithm also provide input for P-wave time imaging and geometrical-spreading correction in layered orthorhombic media.

Introduction

The nonhyperbolic moveout of P-waves in orthorhombic media is governed by the azimuth φ of one of the vertical symmetry planes, the NMO velocities ($V_{\text{nmo}}^{(1)}$ and $V_{\text{nmo}}^{(2)}$) in the symmetry-plane directions, and three anisotropic “anellipticity” coefficients ($\eta^{(1,2,3)}$). Since both the ratio of the symmetry-plane NMO velocities and the η coefficients for fracture-induced orthorhombic models are sensitive to the fracture compliances and orientations (Bakulin et al., 2000), nonhyperbolic moveout inversion can help in building physical models for reservoir characterization. As shown by Grechka and Tsvankin (1999b), the parameters $V_{\text{nmo}}^{(1,2)}$ and $\eta^{(1,2,3)}$ are responsible for all time-processing steps for orthorhombic anisotropy, including NMO correction, dip-moveout (DMO) removal, and time migration. Therefore, the moveout parameters estimated from long-spread moveout can also be used in time imaging of P-wave data from orthorhombic formations.

The goal of this paper is to develop a practical methodology for the inversion of P-wave nonhyperbolic moveout for layered orthorhombic media. We use the generalized form of the Alkhalifah-Tsvankin (1995) moveout equation suggested by Xu et al. (2003) to invert for the orientation of the symmetry planes and five moveout parameters from 3D wide-azimuth, long-spread data.

Nonhyperbolic moveout equation

The nonhyperbolic moveout equation for VTI (transversely isotropic with a vertical symmetry axis) media expressed in terms of V_{nmo} and η (Alkhalifah and Tsvankin, 1995) can be applied to a horizontal orthorhombic layer by making both parameters functions of azimuth (Xu et al., 2003):

$$t^2(x) = t_0^2 + \frac{x^2}{V_{\text{nmo}}^2(\alpha)} - \frac{2\eta(\alpha)x^4}{V_{\text{nmo}}^2(\alpha)[t_0^2V_{\text{nmo}}^2(\alpha) + (1 + 2\eta(\alpha))x^2]}; \quad (1)$$

$$V_{\text{nmo}}^{-2}(\alpha) = \frac{\sin^2(\alpha - \varphi)}{[V_{\text{nmo}}^{(1)}]^2} + \frac{\cos^2(\alpha - \varphi)}{[V_{\text{nmo}}^{(2)}]^2}; \quad (2)$$

$$\eta(\alpha) = \eta^{(2)} \cos^2(\alpha - \varphi) - \eta^{(3)} \cos^2(\alpha - \varphi) \sin^2(\alpha - \varphi) + \eta^{(1)} \sin^2(\alpha - \varphi), \quad (3)$$

where α is the source-to-receiver azimuth with respect to the acquisition frame, and φ is the azimuth of the $[x_1, x_3]$ symmetry plane of the orthorhombic medium (we assume that one of the symmetry planes is horizontal). While equation (2) for the NMO ellipse is exact even for arbitrary anisotropy and heterogeneity, equation (3) is based on the weak-anisotropy approximation for a single orthorhombic layer. We found that equation (3) remains sufficiently accurate for a stack of horizontal orthorhombic layers with a uniform orientation of the vertical symmetry planes.

If the azimuths of the symmetry planes vary with depth, it is necessary to account for the possible misalignment of the NMO ellipse with the “principal axes” of the function $\eta(\alpha)$. Xu and Tsvankin (2004) demonstrate that this can be accomplished by simply replacing the angle φ in equation (3) with a separate azimuth (φ_1) responsible for the

azimuthal variation of the effective parameter η ,

$$\begin{aligned} \eta(\alpha) &= \eta^{(2)} \cos^2(\alpha - \varphi_1) \\ &- \eta^{(3)} \cos^2(\alpha - \varphi_1) \sin^2(\alpha - \varphi_1) + \eta^{(1)} \sin^2(\alpha - \varphi_1). \end{aligned} \quad (4)$$

Inversion algorithm

Our parameter-estimation algorithm is designed to estimate the azimuth φ (and possibly φ_1) and the parameters $V_{\text{nmo}}^{(1)}$, $V_{\text{nmo}}^{(2)}$, $\eta^{(1)}$, $\eta^{(2)}$, and $\eta^{(3)}$ using the moveout equation (1). We follow the approach of Grechka and Tsvankin (1999a) who suggested to reconstruct the NMO ellipse by processing all traces for a given superbin simultaneously using a 3D semblance operator. To aid the efficiency of the algorithm, the full 3D semblance search for the best-fit model is preceded by two preliminary parameter-estimation steps designed to find approximate values of all model parameters except for $\eta^{(3)}$. First, we mute long offsets and apply the algorithm of Grechka and Tsvankin (1999a) to reconstruct the best-fit NMO ellipse for each reflection event. The orientation and semi-axes of the NMO ellipse yield the initial values for the symmetry-plane orientation (angle φ) and velocities $V_{\text{nmo}}^{(1)}$ and $V_{\text{nmo}}^{(2)}$. Second, we perform 2D nonhyperbolic moveout inversion in two narrow azimuthal sectors aligned with the identified symmetry-plane directions to estimate the parameters $\eta^{(1)}$ and $\eta^{(2)}$, which govern long-spread moveout in the planes $[x_2, x_3]$ and $[x_1, x_3]$, respectively. Finally, 3D semblance optimization is applied to invert for all six parameters using the full range of offsets and azimuths.

If the model includes layers with depth-varying azimuths of the symmetry planes, the only change in the inversion methodology described above is that the 3D semblance search (i.e., the last inversion step) is carried out using equation (4) instead of equation (3). While estimating φ_1 , we hold the orientation of the NMO ellipse (i.e., the azimuth φ) constant.

Tests on synthetic data

Single orthorhombic layer

The first test is performed for a single horizontal orthorhombic layer using synthetic data generated by anisotropic ray tracing. Although the algorithm in this noise-free test was able to converge toward the correct model, it is important to identify possible tradeoffs among the medium parameters by studying the shape of the objective function. To quantify such tradeoffs, we hold four model parameters at the correct values and compute the objective function near the actual solution as a function of the remaining two parameters.

Figure 1a shows the semblance scan over the parameters $V_{\text{nmo}}^{(2)}$ and $\eta^{(2)}$ computed from equation (1) using the correct values of φ , $V_{\text{nmo}}^{(1)}$, $\eta^{(1)}$, and $\eta^{(3)}$. Despite the large

maximum offset-to-depth ratio ($x/z = 3$), there exists a family of models with a range of $\eta^{(2)}$ values that fit the data. The tradeoff between $V_{\text{nmo}}^{(2)}$ and $\eta^{(2)}$ has the same character as the interplay between V_{nmo} and η in VTI media (Grechka and Tsvankin, 1998). Since the parameter $\eta^{(3)}$ has no influence on reflection traveltimes near both symmetry planes, it is resolved more poorly than is $\eta^{(2)}$ (Figure 1b). The ambiguity in all η parameters increases for smaller offset-to-depth ratios. In contrast, the inversion algorithm yields a highly accurate estimate of the azimuth φ (Figure 1c) because the orientation of the symmetry planes can be inferred from both the NMO ellipse and azimuthally varying nonhyperbolic moveout.

Layered anisotropic media

If the medium above the reflector is multilayered, the moveout coefficients become effective quantities that incorporate the influence of both anisotropy and vertical heterogeneity. The model in Figure 2a includes an orthorhombic layer overlain by a VTI layer of equal thickness. Because of the smaller contribution of the moveout in the azimuthally anisotropic layer to the total traveltime, the resolution of the symmetry-plane azimuth φ is lower than that for a homogeneous medium. In general, the accuracy in estimating the symmetry-plane orientation depends on the relative thickness (i.e., on the ratio of the thickness and depth) of the azimuthally anisotropic layer.

Next, we applied the inversion algorithm to a two-layer orthorhombic model with misaligned symmetry planes (Figures 2b,c). The estimated azimuth φ obtained using equation (3) (Figure 2b) corresponds to a direction that is somewhat closer to the $[x_1, x_3]$ symmetry plane in the top layer. The semblance value for the best-fit model (0.69) is much lower than the semblances obtained for the two previous models. Replacing equation (3) by equation (4) helps to increase the value of semblance by about 20% which is indicative of a better traveltime fitting ensured by decoupling the orientation of the NMO ellipse from that of the function $\eta(\alpha)$. Note that the azimuth φ_1 in Figure 2c moves closer to the $[x_1, x_3]$ symmetry plane of the bottom layer. In general, the effective value of φ_1 is determined by the relative thicknesses, symmetry-plane orientations, and moveout parameters of the constituent layers. Since the azimuth φ_1 influences only nonhyperbolic moveout, it is not as well resolved as is φ (Figures 2b,c).

Field-data example

We applied the moveout inversion algorithm to wide-azimuth data acquired at Weyburn Field located in the Williston basin in Canada. This multicomponent data set was processed and interpreted by the Reservoir Characterization Project at Colorado School of Mines with the main goal of dynamic monitoring of the CO₂ flood in the fractured reservoir. Jenner (2001) identified the

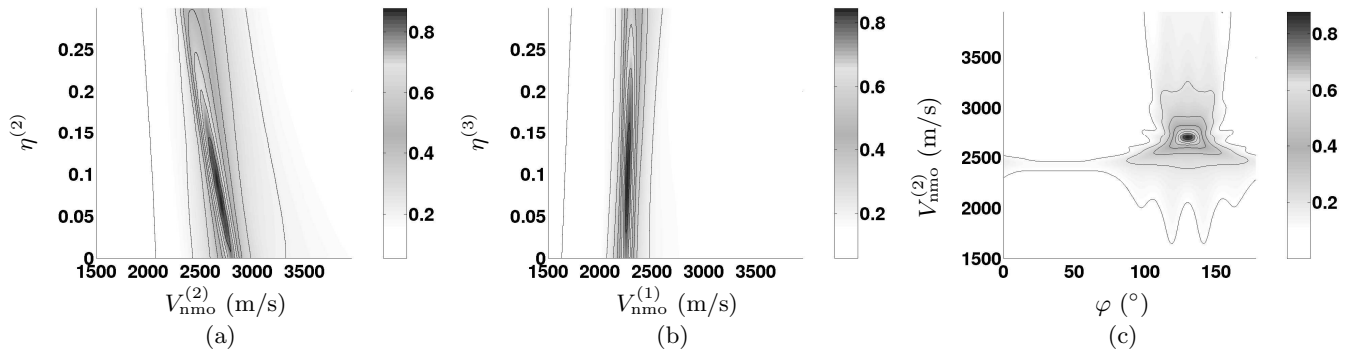


Fig. 1: Semblance scans over different pairs of the medium parameters computed for a single orthorhombic layer using equation (1). (a) $V_{\text{nmo}}^{(2)}$ and $\eta^{(2)}$; (b) $V_{\text{nmo}}^{(1)}$ and $\eta^{(3)}$; (c) φ and $V_{\text{nmo}}^{(2)}$. The maximum offset-to-depth ratio $x/z = 3$. The true model parameters are $\varphi = 130^\circ$, $V_{\text{nmo}}^{(1)} = 2269$ m/s, $V_{\text{nmo}}^{(2)} = 2699$ m/s, $\eta^{(1)} = 0.196$, $\eta^{(2)} = 0.065$, and $\eta^{(3)} = 0.094$.

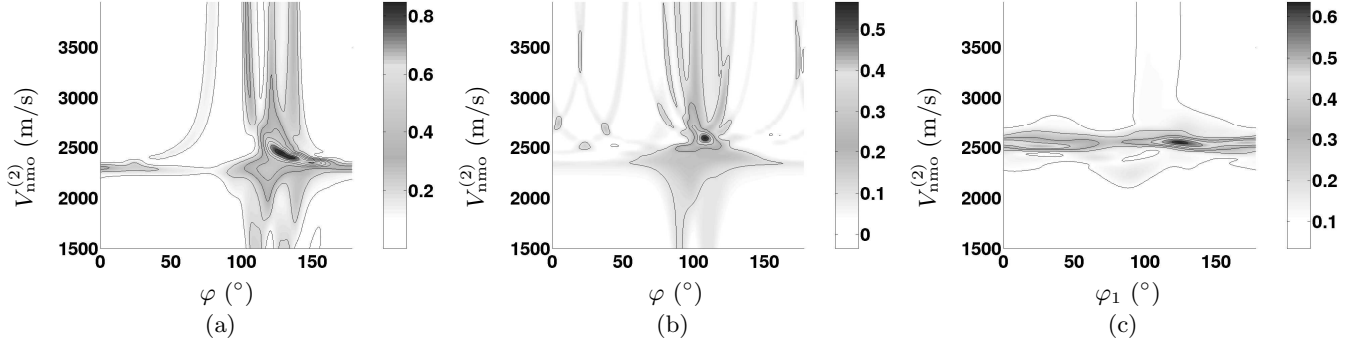


Fig. 2: Semblance scans for the reflection from the bottom of a model composed of two layers with equal thickness. The orthorhombic layer from Figure 1 is overlain by (a) VTI layer with $V_{\text{nmo}} = 2158$ m/s and $\eta = 0.196$; (b,c) orthorhombic layer with a different orientation of the symmetry planes ($\varphi = 90^\circ$) and the parameters $V_{\text{nmo}}^{(1)} = 2156$ m/s, $V_{\text{nmo}}^{(2)} = 2534$ m/s, $\eta^{(1)} = 0.398$, $\eta^{(2)} = 0.211$, and $\eta^{(3)} = 0.193$. The parameter estimation was performed using equation (3) for plots (a) and (b) and equation (4) for plot (c).

presence of laterally varying azimuthal anisotropy at the reservoir level by computing the interval P-wave NMO ellipses and performing azimuthal AVO (amplitude variation with offset) analysis. Another reliable indicator of azimuthal anisotropy is shear-wave splitting at near-vertical incidence, which was studied at Weyburn field by Cardona (2002). According to Cardona's (2002) results, the magnitude of shear-wave splitting is not negligible throughout most of the section.

The 3D nonhyperbolic moveout inversion [using equation (3)] was applied to P-waves collected into 9x9 superbins, one of which is centered at CMP 10103 and another at CMP 10829 (Figure 3). Because of the limited offset range, we were able to process only the reflections from several horizons above the reservoir. The anisotropy in most of the overburden is quite substantial, with η values reaching 0.25 for the reflection from the deepest interface (the Mississippian unconformity). The resolution in the anellipticity parameters decreases for the lower horizons because of the smaller offset-to-depth ratio. The symmetry-plane azimuth φ is not well-constrained even for the shallow horizons, which likely results from a relatively small magnitude of azimuthal anisotropy. To verify whether it is possible to fit the data without taking azimuthal anisotropy into account, we ran the inversion algorithm for VTI media and observed a measurable (10% on average) reduction in semblance.

Another indication of the influence of azimuthal anisotropy on reflection moveout is the consistency of

estimated symmetry-plane azimuth φ for all four reflection events at a fixed CMP location. Although the values of φ differ from CMP 10103 to CMP 10829, both symmetry-plane orientations are close to the directions of the off-trend fracture sets obtained from borehole data (Cardona, 2002). Although the anellipticity parameters represent effective values for the stack of layers above the reflector, they still provide useful information about the vertical variation in the magnitude and character of the anisotropy.

Discussion and conclusions

We applied a modified version of the nonhyperbolic moveout equation of Alkhalifah and Tsvankin (1995) to invert for the P-wave moveout parameters of orthorhombic media from wide-azimuth, long-offset data. This equation adequately describes reflection traveltimes for layered orthorhombic models with a uniform orientation for the symmetry planes. Since the the symmetry-plane azimuth φ and the NMO velocities $V_{\text{nmo}}^{(1)}$ and $V_{\text{nmo}}^{(2)}$ define the NMO ellipse, they are constrained better than are the anellipticity parameters $\eta^{(1)}$, $\eta^{(2)}$, and $\eta^{(3)}$, which make a significant contribution to the traveltimes only for large offset-to-depth ratios (e.g., $x/z > 2$). As is the case for VTI media, estimation of the η -parameters is hampered by the tradeoffs between $V_{\text{nmo}}^{(1)}$ and $\eta^{(1)}$, and between $V_{\text{nmo}}^{(2)}$ and $\eta^{(2)}$ (Grechka and Tsvankin, 1998b). These tradeoffs can cause substantial uncertainties in

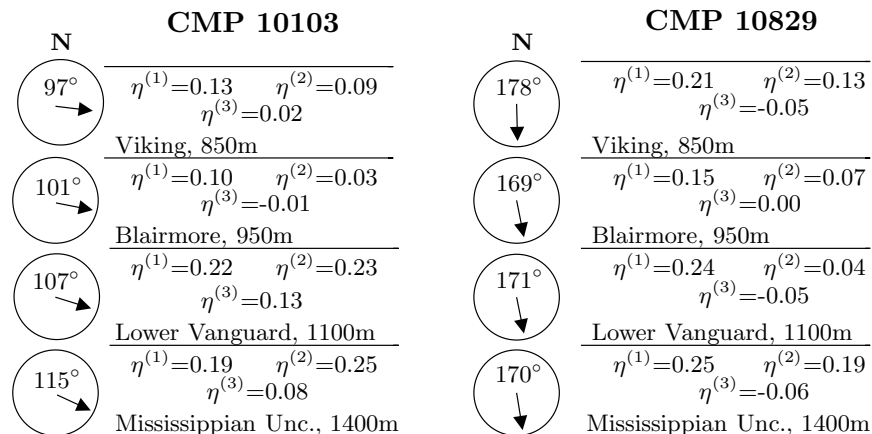


Fig. 3: Inversion results for the reflections from (a) the Viking horizon, the maximum offset-to-depth ratio $x/z = 2.5$; (b) the Blairmore, $x/z = 2.0$; (c) the Lower Vanguard, $x/z = 1.9$; and (d) the Mississippian Unconformity, $x/z = 1.8$. The arrows mark the estimated direction of the semi-major axis of the NMO ellipse; the number by each arrow is the azimuth of the axis with respect to the north.

$\eta^{(1)}$ and $\eta^{(2)}$ if the data are contaminated by correlated noise and the maximum ratio x/z is smaller than 2.5. The least-constrained model parameter is $\eta^{(3)}$ because it influences only long-spread moveout in off-symmetry directions.

If the orientation of the symmetry planes varies with depth, our moveout equation is less accurate, and the semblance values become smaller. A better moveout approximation for models without throughgoing vertical symmetry planes can be obtained by accounting for the misalignment of the axes of the NMO ellipse and the principal directions of the azimuthally varying parameter η .

Application of our methodology to wide-azimuth P-wave data acquired over a fractured reservoir at Weyburn Field in Canada reveals a substantial magnitude of nonhyperbolic moveout and non-negligible azimuthal anisotropy in the overburden. Because the reflection moveout is largely controlled by polar anisotropy (i.e., by vertical transverse isotropy), the resolution of the symmetry-plane azimuth φ is relatively low. Nevertheless, taking azimuthal anisotropy into account increases the semblance by about 10% and produces consistent values of the azimuth φ for all four horizons used in the analysis. Application of our algorithm to geometrical-spreading correction in layered orthorhombic media is discussed by Xu and Tsvankin (2004).

Acknowledgments

We thank Edward Jenner (currently GMG/Axis) and the Reservoir Characterization Project at CSM for providing the Weyburn Field data and discussing their interpretation results with us.

References

Alkhalifah, T., and Tsvankin, I., 1995, Velocity analy-

sis for transversely isotropic media: *Geophysics*, **60**, 1550–1566.

- Bakulin, A., Grechka, V., and Tsvankin, I., 2000, Estimation of fracture parameters from reflection seismic data—Part II: Fractured models with orthorhombic symmetry: *Geophysics*, **65**, 1803–1817.
- Cardona, R., 2002, Fluid substitution theories and multicomponent seismic characterization of fractured reservoirs: PhD thesis, Colorado School of Mines, 199p.
- Grechka, V., and Tsvankin, I., 1998, Feasibility of nonhyperbolic moveout inversion in transversely isotropic media: *Geophysics*, **63**, 957–969.
- Grechka, V., and Tsvankin, I., 1999a, 3-D moveout velocity analysis and parameter estimation for orthorhombic media: *Geophysics*, **64**, 820–837.
- Grechka, V., and Tsvankin, I., 1999b, 3-D moveout inversion in azimuthally anisotropic media with lateral velocity variation: Theory and a case study: *Geophysics*, **64**, 1202–1218.
- Jenner, E., 2001, Azimuthal anisotropy of 3-D compressional wave seismic data, Weyburn field, Saskatchewan, Canada: PhD thesis, Colorado School of Mines.
- Xu, X., and Tsvankin, I., 2004, Geometrical spreading correction for P-waves in azimuthally anisotropic media: 74th Ann. Internat. Mtg., Soc. Expl. Geophys., Expanded Abstracts.
- Xu, X., Tsvankin, I., and Pech, A., 2003, Geometrical spreading of P-waves in azimuthally anisotropic media: 73rd Ann. Internat. Mtg., Soc. Expl. Geophys., Expanded Abstracts, 801–804.